

3.5 SCCMS Projects

First-Principles Phase Field Mapping

Kaoru Ohno

Department of Physics, Faculty of Engineering Science,

Yokohama National University, Tokiwadai, Hodogaya-ku, Yokohama 240-8501

In order to predict microstructures of alloys without relying on any empirical or experimental parameter, we have developed the first-principles phase field method by combining cluster expansion theory, potential renormalization theory and density functional theory and applied it to NiAl alloys that are used for example in jet engine turbine blades at high temperature [1]. This year, we focused on Ti-6wt%Al-4wt%V (Ti64) alloy, which is one of the most used Ti alloys in industry in a broad range from aerospace to medical applications. The mechanical properties and the phase transformation of Ti64 are strongly influenced by the microstructure, which is reliant on the history of processing, thermal treatment procedures and alloying element partitioning

effects. We succeeded in applying the first-principles phase field method to this system without using any thermodynamic parameter and identifying the element partitioning effect, i.e., enrichment of V in the β grain boundary and Al in the α phase at 977 °C. Figs. 1(a) and (b) show the resulting V and Al concentrations, while Figs. 1(c) and (d) show the corresponding experimental images [3], which look very similar to each other. As a conclusion, the present method has an ability to predict complex microstructure of alloys.

References

- [1] S. Bhattacharyya, R. Sahara, and K. Ohno, Nature Communications **10**, 3451;1-10 (2019).
- [2] T. N. Pham, K. Ohno, R. Kuwahara, and S. Bhattacharyya, J. Phys.: Cond. Mat. **32**, 264001;1-9 (2020).
- [3] S. Huang, et al. J. Alloys Compounds. **791**, 575-585 (2019).

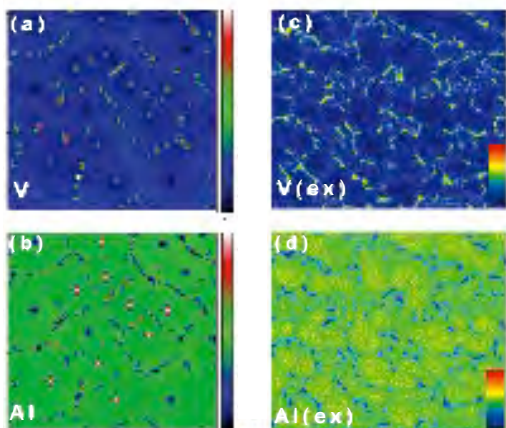


Fig. 1: (a) V and (b) Al concentrations obtained by the present method [2], and (c), (d) the corresponding experimental images [3].

Energy conversion --chemical energy--

Osamu SUGINO

Institute for Solid State Physics,

The University of Tokyo, Kashiwa-no-ha, Kashiwa, Chiba 277-8581

Challenge of electrochemical interface study is to establish a quantum theory of electrode and to predict an ultimately efficient energy conversion. To this end we studied two topics, manifestation of nuclear quantum effect on H/Pt(111) and environmental effect on the oxygen reduction reaction (ORR) on transition metal oxides. The nuclear quantum effect was investigated by applying the first-principles path integral molecular dynamics (PIMD) under different coverage conditions [1]. The hydrogen atoms are known to be delocalized quantum mechanically under low coverage but, with increasing coverage, the interatomic repulsion is found to induce localization within an adsorption site; atop, fcc, or hcp. The interaction induced localization, which had been shown to exist in a low index noble metal surfaces, was captured on platinum and this phenomenon is found to

provide a hint to the hitherto unexplained structure of H/Pt(111).

It is also important to utilize the simulation for electrocatalyst design. Platinum alloys are used in the existing fuel cells, but they are not active enough. For better electrocatalysts, transition metal oxides are attracting attention, but the mechanism has not been understood. In collaboration with experimental groups, we calculated the correlation of the adsorption energies of the ORR intermediates, O_2H , OH , and O ; the correlation is known to be a descriptor of the activity. For most materials, the correlation curve does not cross the point for ideal activity, but TiO_2 and ZrO_2 are found to cross it when doped with some noble metal dopants [2]. The activity versus defects relation is consistent with experimental findings. From these results, the joint research group is now planning to realize an ideal

catalyst.

C123 19486 (2019).

References

- [1] L. Yan et al. Phys. Rev. B101, 165414 (2020).
- [2] Y. Yamamoto et al. J. Phys. Chem.

Molecular Dynamics Simulation Studies of Electrochemical Properties of Ionic Liquid Electrolytes

Hayato SHIBA^{1,2} and Patrick A. BONNAUD¹

¹*Institute for Materials Research, Tohoku University, Katahira, Aoba-ku, Sendai 980-8577*

²*Information Technology Center, The University of Tokyo, Kashiwa-no-ha, Kashiwa, Chiba 277-8589*

Ionic liquids (ILs) are salts that are liquid at the good reason that they are composed only of ions, they are expected to be good candidates for electrolytes in supercapacitors. They may exhibit fast charging times, excellent power performances, and good aging properties. In this project, we focused on capacitors based on properties of Electrical Double Layer Capacitors (EDLC), in which ionic liquid are confined between a pair of planar electrodes.

We employed molecular simulation to study underlying molecular mechanisms of electrical properties in EDLC. we selected an ionic pair widely studied experimentally: 1-butyl-3-methylimidazolium / bis[(trifluoromethyl) sulfonyl] imide. Then, we inserted those ions in a simulation box made of two electrodes separated by a slit-shape gap of 4 and 6 nm up to a mass density corresponding to given thermodynamics conditions ($300 < T < 400$ K and $p \sim 1$ atm). We employed LAMMPS in combination with the constant potential method to simulate EDLC at the molecular scale, by using a subroutine by Zhenxing Wang *et al.*¹

We have observed that ions migrate toward electrodes of opposite charge upon an applied voltage. The fluid structure in vicinal layers that span over roughly 1 nm with respect to the electrode surface is more pronounced than in the neutral state. In the core of the gap between electrodes, the higher the applied voltage, the more structured the fluid. Ions formed alternative layers of cations and anions. From the average total charge sampled on one of the electrodes, we computed the total gravimetric capacitance and observed a fast increase at low applied voltages before reaching a nearly constant behavior beyond 1V. Those results set a cornerstone for the understanding of molecular mechanisms underlying electrical properties of EDLC.

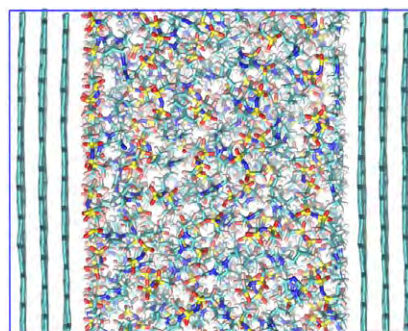


Fig. 1: Snapshot of a molecular model for simulations at constant potential.

¹ <https://github.com/zhenxingwang/lammps-conp>

Development of accuracy verification method on analytic continuation results using cross validation

Kazuyoshi YOSHIMI¹, Yuichi MOTOYAMA¹, Yoshinori NAKANISHI-OHNO²

¹*Institute for Solid State Physics, University of Tokyo, Kashiwa 277-8581*

²*Graduate School of Arts and Sciences, University of Tokyo, Tokyo, 153-8902*

Recent developments in computational sciences have made it possible to construct and analyze effective models for realistic materials. Quantum Monte Carlo (QMC) calculations are one of powerful methods for finite temperature analysis of effective models. To compare with experimental results such as excitation spectra, it is necessary to connect the results of imaginary time simulations in QMC method to real time by means of a numerical analytic continuation. However, there is a problem that small statistical noise of the input data has a great influence on the results of the analytic continuation, and there has been no decisive method to enable high-precision spectral analysis until now.

Recently, we have proposed a method to automatically select bases which are insensitive to noise using sparse modeling and to achieve a numerically stable analytic continuation against noise (SpM) [1-3]. In addition, SpM can easily add physically required conditions as constraints, such as spectral non-negativity and sum rule. In this work, we have developed a new method to improve the validity of the results obtained by SpM. We also developed software to enable the

verification on the results obtained by SpM using cross-validation.

In SpM, artificial oscillations appear in the low frequency range due to the cutoff of the bases. To solve this problem, we focused on the Pade approximation, which gives high-precise analytic continuation in the low-frequency region. In our method (SpM-Pade), the cost function which becomes large when the difference between the spectrum and that by Pade becomes large in the region where the spectrum by Pade is stable to noise. We

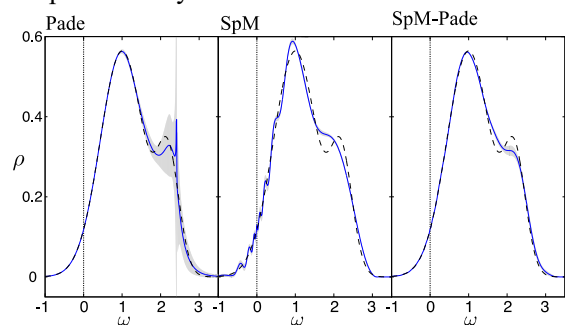


Figure 1 Reconstructed spectrum by the Pade (left), the SpM (center), and the SpM-Pade (right) method. The line denotes the mean value and the shaded region denotes the standard deviation from 30 independent samples. The exact spectrum is shown as the black dashed line.

examined the validity of SpM-Pade using the test data obtained by adding noise to the artificially given spectrum and performing an inverse transformation of the analytic continuation. In order to see the sensitivity to noise, the simulations were done for 30 independent samples. In Fig. 1, we show the reconstructed spectrum by the Pade (left), the SpM (center), and the SpM-Pade (right) methods, respectively. It is seen that using Pade approximation, the spectrum (solid line) is almost same as the exact one (dashed line) around $\omega=0$ and the standard deviation (shaded area) is small. With increasing ω , both the difference between the spectrum and the exact one and the deviation become large toward the second peak around $\omega=2$ as expected. In the case of SpM, the oscillations appear around $\omega=0$ and the second peak becomes broad compared to the exact one. However, the small variance indicates that this method is insensitive to noise. In the case of SpM-Pade, due to introducing the cost function, the oscillations around $\omega=0$ is suppressed. On the other hand, the noise tolerance is still strong as seen from the small

deviation. Actual data, such as QMC data, have a correlation between imaginary time data. In the current simulation, we have ignored these effects. We plan to apply SpM-Pade to the QMC data and investigate its applicability.

For the cross-validation program, we develop a program for large-scale parallel computers so that it is designed not only to be used for analytic continuation but also for various methods. Now, we confirmed that it worked on the ISSP supercomputer for the analysis in which the reduction of the noise of the image was done using sparse modeling. We plan to release this program as open source software when it can be used for various solvers, including the program of SpM [2].

References

- [1] J. Otsuki, M. Ohzeki, H. Shinaoka, and K. Yoshimi: Phys. Rev. E **95** (2017) 061302.
- [2] K. Yoshimi J. Otsuki, Y. Motoyama, M. Ohzeki, and H. Shinaoka: Comput. Phys. Commun. **244** (2019) 319.
- [3] J. Otsuki, M. Ohzeki, H. Shinaoka, and K. Yoshimi: J. Phys. Soc. Jpn. **89** (2020) 2061.

Ab initio study of quantum spin liquid in molecular conductors

Takahiro Misawa

Institute for Solid State Physics, University of Tokyo
Kashiwa-no-ha, Kashiwa, Chiba 277-8581

It has been experimentally reported that the $X[\text{Pd}(\text{dmit})_2]_2$ molecular conductors exhibit various phases such as antiferromagnetic, spin-liquid, and charge-ordered states depending on the choice of cation (X) [1]. In order to elucidate the origin of this variety of phenomena, detailed analyzes of band structures and transfer integrals based on the extended Hückel method and first-principles calculations have been performed to quantitatively evaluate the material dependence of electronic states [2]. On the other hand, systematic analyses incorporating the electron correlation effect, which plays an important role in the emergence of various phases, have not been carried out due to the lack of efficient tools and the need for large computational resources for analysis in molecular conductors. We note that the derivation of the low-energy effective Hamiltonian including the interaction parameters is carried out only for $\text{EtMe}_3\text{Sb}[\text{Pd}(\text{dmit})_2]_2$ [3], which has the quantum spin liquid ground state.

In this project, using the open-source software package RESPACK [4, 5], we systematically derive effective Hamiltonians for all available nine $\beta'-X[\text{Pd}(\text{dmit})_2]_2$ ($X = \text{Me}_4\text{Y}$, EtMe_3Y , $\text{Et}_2\text{Me}_2\text{Y}$ and , $Y = \text{As}$, Sb , and P) [6]. In the part of obtaining the global band structures, we use Quantum ESPRESSO [7]. Furthermore, using the quantum lattice model solver $\mathcal{H}\Phi$ [8, 9], we perform the numerically exact analyzes for the obtained low-energy effective Hamiltonians and show that the mag-

netic properties are well reproduced including the quantum spin liquid behavior observed in $X=\text{EtMe}_3\text{Sb}$. We also show that both the geometrical frustration and the off-site interactions play key role in stabilizing the quantum spin liquid.

In addition to the *ab initio* study for the molecular conductors, we perform the *ab initio* calculations for the high- T_c cuprates [10, 11]. We also analyze the quantum transport phenomena in the Weyl semimetals [12] and the topological semimetals [13] using the real-time evolution of the quantum systems. Furthermore, using the many-variable variational Monte Carlo method [14, 15], we analyze the quantum spin-nematic phase [16], the Kitaev model under magnetic fields [17], and the dynamical properties of the correlated electron systems [18].

References

- [1] R. Kato, Chem. Rev. **104**, 5319 (2004).
- [2] K. Kanoda, R. Kato, Annu. Rev. Condens. Matter Phys. **2**, 167 (2011).
- [3] K. Nakamura, Y. Yoshimoto, M. Imada, Phys. Rev. B **86**, 205117 (2012).
- [4] <https://sites.google.com/view/kazuma7k6r>
- [5] K. Nakamura, Y. Yoshimoto, Y. Nomura, T. Tadano, M. Kawamura, T. Kosugi,

- K. Yoshimi, T. Misawa, Y. Motoyama,
arXiv preprint arXiv:2001.02351.
- [6] T. Misawa, K. Yoshimi, T. Tsumuraya,
arXiv preprint arXiv:2004.00970.
- [7] P. Giannozzi, O. Andreussi, T. Brumme,
O. Bunau, M. B. Nardelli, M. Calandra,
R. Car, C. Cavazzoni, D. Ceresoli, M. Co-
coccioni, et al., *Journal of Physics: Con-
densed Matter* **29**, 465901 (2017).
- [8] M. Kawamura, K. Yoshimi, T. Misawa,
Y. Yamaji, S. Todo, N. Kawashima, *Com-
put. Phys. Commun.* **217**, 180 (2017).
- [9] [https://www.pasums.issp.u-tokyo.
ac.jp/HPhi/en/](https://www.pasums.issp.u-tokyo.ac.jp/HPhi/en/)
- [10] M. Hirayama, T. Misawa, T. Ohgoe,
Y. Yamaji, M. Imada, *Phys. Rev. B* **99**,
245155 (2019).
- [11] T. Ohgoe, M. Hirayama, T. Misawa,
K. Ido, Y. Yamaji, M. Imada, *Phys. Rev.
B* **101**, 045124 (2020).
- [12] T. Misawa, R. Nakai, K. Nomura, *Phys.
Rev. B* **100**, 155123 (2019).
- [13] T. Misawa, K. Nomura, *Scientific Reports*
9, 19659 (2019).
- [14] T. Misawa, S. Morita, K. Yoshimi,
M. Kawamura, Y. Motoyama, K. Ido,
T. Ohgoe, M. Imada, T. Kato, *Comput.
Phys. Commun.* **235**, 447 (2019).
- [15] [https://www.pasums.issp.u-tokyo.
ac.jp/mvmc/en/](https://www.pasums.issp.u-tokyo.ac.jp/mvmc/en/)
- [16] T. Hikihara, T. Misawa, T. Momoi, *Phys.
Rev. B* **100**, 214414 (2019).
- [17] K. Ido, T. Misawa, *Phys. Rev. B* **101**,
045121 (2020).
- [18] K. Ido, M. Imada, T. Misawa, *Phys. Rev.
B* **101**, 075124 (2020).

Unified Photonic-Electronic Devices

Kazuhiro YABANA

Center for Computational Sciences,

University of Tsukuba, Tsukuba 305-8577

We develop a first-principles computational method to investigate electron dynamics induced by ultrashort laser pulses based on time-dependent density functional theory (TDDFT) in real time. We develop the code SALMON (Scalable Ab-initio Light-Matter simulator for Optics and Nanoscience) [1] and make it open to the public at our website, <http://salmon-tddft.jp>.

SALMON is developed as a unified software that include traditional computational methods of light-matter interaction, the electromagnetism analysis using finite-difference time-domain (FDTD) method, and linear response calculation for susceptibilities based on TDDFT. There are two options for the coupling: macroscopic[2] and microscopic [3]. In addition, Ehrenfest molecular dynamics can be combined in the multiscale simulation [4].

This year, we have concentrated on the development of ver. 2 of SALMON. In the new version, we intended to improve the readability and extensibility of the code by using structures of Fortran extensively. We also paid much effort to improve the efficiency and scalability for large-scale calculations. Using the code, it is

now possible to calculate the ground state and electron dynamics of systems of more than a few thousand atoms. We intend to make the new version public in early fiscal year of 2020.

References

- [1] M. Noda, et.al, “SALMON: Scalable Ab-initio Light–Matter simulator for Optics and Nanoscience”, *Comp. Phys. Comm.* 235, 356 (2019).
- [2] K. Yabana, T. Sugiyama, Y. Shinohara, T. Otobe, G.F. Bertsch, “Time-dependent density functional theory for strong electromagnetic fields in crystalline solids”, *Phys. Rev. B* 85, 045134 (2012).
- [3] S. Yamada, M. Noda, K. Nobusada, K. Yabana, “Time-dependent density functional theory for interaction of ultrashort light pulse with thin materials”, *Phys. Rev. B* 98, 245147 (2018).
- [4] A. Yamada, K. Yabana, “Multiscale time-dependent density functional theory for a unified description of ultrafast dynamics: Pulsed light, electron, and lattice motion in crystalline solids”, *Phys. Rev. B* 99, 245103 (2019).

Dynamical DMRG study of magnetic excitations in magnetization plateaus of a frustrated spin ladder

Takami TOHYAMA

Department of Applied Physics, Tokyo University of Science, Tokyo 125-8585

Magnetization plateau (MP) emerges in quantum spin systems due to spontaneously breaking of translational symmetry. The broken symmetry can induce reconstruction of elementary excitations, but its microscopic mechanism and reconstructed quasiparticle in MP phases have remained unclear. We theoretically study magnetic excitations in the MP phases of a frustrated spin ladder (FSL) by using the dynamical density-matrix renormalization-group (DDMRG) method [1].

The Hamiltonian of FSL is defined as $H = H_{\perp} + H_{\parallel} + H_Z$ with $H_{\perp} = J_{\perp} \sum_{i=1}^N \mathbf{S}_{i,1} \cdot \mathbf{S}_{i,2}$, $H_{\parallel} = \sum_{\eta=1}^2 J_{\eta} \sum_i \sum_{j=1}^2 \mathbf{S}_{i,j} \cdot \mathbf{S}_{i+\eta,j}$, and $H_Z = -h \sum_{i,j} S_{i,j}^z$, where $\mathbf{S}_{i,1}$ ($\mathbf{S}_{i,2}$) is the $S = 1/2$ spin operator on i th rung in the upper (lower) chain. Exchange energies of the first-neighbor bond in a leg, the second-neighbor bond in a leg, and the first-neighbor bond in a rung, are denoted by J_1 , J_2 , and J_{\perp} , respectively. We set $J_1/J_{\perp} = 0.2$ and $J_2/J_{\perp} = 0.65$. Changing magnetic field h , we obtain MPs at $m = M/M_s = 1/3, 1/2$, and $2/3$, where M (M_s) is magnetization (saturation magnetization).

We calculate dynamical spin structure factor (DSSF) using DDMRG, where the correction vector is expanded by the Legendre polynomial with a Gaussian averaging [2] and a broadening factor is replaced by the width of the Gaussian, for which we set $0.02J_{\perp}$. The system size, $N = 48$ rungs, is sufficient to discuss dynamical behaviors. The number of states kept in the DDMRG is $m = 600$, leading to truncation error less than 1×10^{-4} .

Figure 1 shows DSSF for momentum along

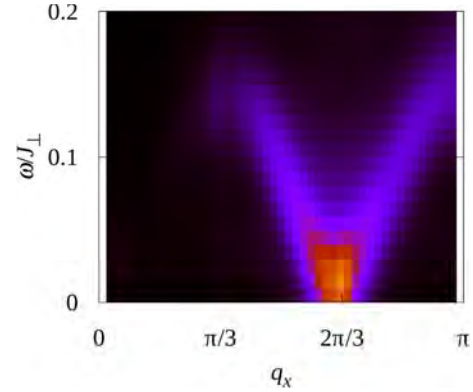


Figure 1: DSSF for $q_y = \pi$ in the $m = 1/3$ MP.

rung $q_y = \pi$ as a function of momentum along leg q_x in the case of $m = 1/3$ [1]. A dispersive feature with zero-energy excitation at $q_x = 2\pi/3$, indicating a period with three times the original unit-cell length in real space.

We also perform analytical approaches with the perturbation theory to obtain an intuitive view of magnetic excitations. A comparison between numerical and analytical results indicates the presence of a reconstructed quasiparticle originating from spontaneously broken translational symmetry, which is realized as a collective mode of the spin trimer called a trimeron [1].

References

- [1] K. Sasaki, T. Sugimoto, T. Tohyama, and S. Sota: Phys. Rev. B **101** (2020) 144407.
- [2] S. Sota and T. Tohyama: Phys. Rev. B **82** (2010) 195130.

Conversion and storage of energy—fuel cells and secondary batteries: Research and development of fundamental technologies of battery simulators.

Susumu OKAZAKI

*Department of Materials Chemistry, Nagoya University
Furo-cho, Chikusa-ku, Nagoya 464-8603*

The goal of our project is to develop the basic technology of the whole battery simulator. One of the key techniques is molecular-level design of polymer membranes controlling transportation of protons and ions across the membrane with proper stiffness resistant to mechanical deformation under external stress. Such membranes are widely applicable to the fuel cells used in the industrial products.

We previously performed fully atomistic molecular dynamics (MD) calculations of hydrated perfluorosulfonic acid (PFSA) ionomers composed of a hydrophobic polytetrafluoroethylene backbone with hydrophilic side chains terminated by sulfonic acid, as a model of proton exchange polymer electrolyte membrane of fuel cells[1, 2, 3]. On the system B and C, we further performed a series of MD calculations of different equivalent weight PFSA membranes containing H₂ molecules at different water uptakes[4] (examples are shown in Figs. 1 (A)–(C)). They explored atomistic detail of H₂ permeation through the membranes. The local semicrystalline structure of the PFSA polymer and the morphology of the water clusters in the membrane were found to affect H₂ permeation.

Moreover, new algorithms relating to the fast multipole method which enable to treat two dimensional periodic boundary conditions (slab geometry)[5] and rectangular unit cell with an anisotropic cell-partitioning[6] were developed. They make it possible to perform

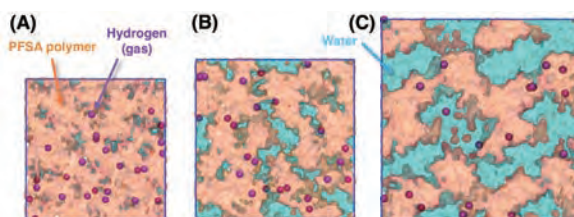


Figure 1: Schematic images of hydrated equivalent weight PFSA membranes with (A) 6, (B) 16, and (C) 30 wt % of water uptakes[4].

MD calculations for more general calculation systems by the software MODYLAS.

These results will contribute to the development of higher performance fuel-cells and secondary batteries and to the realization of the entire battery simulator in the near future.

References

- [1] A. T. Kuo, W. Shinoda, S. Okazaki : *J. Phys. Chem. C* **120** (2016) 25832.
- [2] A. T. Kuo, S. Okazaki, W. Shinoda : *J. Chem. Phys.* **147** (2017) 094904.
- [3] A. T. Kuo, K. Takeuchi, A. Tanaka, S. Urata, S. Okazaki, and W. Shinoda : *Polymer* **146** (2018) 53.
- [4] K. Takeuchi, A. Kuo, T. Hirai, T. Miyajima, S. Urata, S. Terazono, S. Okazaki, and W. Shinoda: *J. Phys. Chem. C*, **123** (2019) 20628.
- [5] N. Yoshii, Y. Andoh, S. Okazaki: *J. Comput. Chem.*, **41** (2020) 940.
- [6] Y. Andoh, N. Yoshii, S. Okazaki: *J. Comput. Chem.*, **41** (2020) 1353.

Development of Fragment-Based GW/BSE Method and Application to Organic Optoelectronic Materials

Takatoshi Fujita

*Institute for Molecular Science
Myodaiji, Okazaki, Aichi 444-8585*

Accurate calculations of electronic states are essential for computational studies of organic materials which are directed toward understanding of fundamental processes in organic electronic devices. Many fundamental processes governing the device operation take place at the variety of interfaces, such as metal-organic and organic donor-acceptor interfaces. Although developments of quantum chemistry or ab initio program packages have enabled one to routinely run a calculation for an isolated molecule or a molecular crystal, performing such a calculation for interface systems is still a challenging issue.

We have recently developed the large-scale GW method [1, 2] which can be applied to large and disordered molecular systems. Our implementation is based on the fragment molecular orbital (FMO) method, in which an entire system is first divided into many subsystems referred as fragments, and total energy or physical properties are approximated from molecular orbital calculations for fragment monomers, dimers, and optionally, trimmers. In the FMO-GW method, the polarization function of an entire system is approximated from molecular orbital localized within fragment monomer or dimers. In addition, the Δ COHSEX approximation is employed, in which dynamically-screened Coulomb potential is explicitly evaluated for a target fragment, while the statically-screened Coulomb potential of entire system is evaluated at the static COHSEX level. Based

on these development, we have performed the large-scale GW calculation for systems which contain more than 1,000 atoms, such as the organic semiconductor thin film [1] and the donor/acceptor interface [2]. In addition, we have also developed the GW/Bethe-Salpeter equation method which reasonably describes excited states in polarizable molecular environments.

As applications of the FMO-GW, we have explored the energy levels and charge-transfer excited states in pentacene/C₆₀ bilayer heterojunctions. In particular, we have investigated the dependence of interfacial morphologies on the electronic states and the effects of polarization and delocalization effects. Calculated energy levels and the excitation energies of charge-transfer states are in reasonable agreement with those estimated from ultraviolet photoelectron spectroscopy and from external quantum efficiency measurements. We have found that the electrostatic contribution of polarization energies, which arises from pentacene quadrupole moments, governs dependence of interfacial morphologies on the electronic states.

References

- [1] T. Fujita, Y. Noguchi, *Phys. Rev. B* **98** (2018) 205140.
- [2] T. Fujita, Y. Noguchi, T. Hoshi, *J. Chem. Phys.* **151** (2019) 114109.

Data-driven materials design for new functional high entropy alloys

Tetsuya Fukushima

*Institute for Solid State Physics, University of Tokyo
Kashiwa-no-ha, Kashiwa, Chiba 277-8581*

Recently, the constructions of materials databases using first-principles calculations have been actively carried out. Combining such materials databases and data-mining technique, one can not only analyze the mechanisms of physical phenomena, but also design new functional materials. Actually, there are several large materials databases, such as Materials Project, Open Quantum Materials Database (OQMD), and Novel Materials Discovery (NOMAD), which researchers can freely access. However, these inorganic materials databases are only for compounds with stoichiometric compositions and do not contain information about configurational disordered systems

In this year, in order to construct the materials databases for configurational disordered systems, we have developed an automatic high-throughput calculation method on the basis of the Korringa-Kohn-Rostoker (KKR) Green's function method. There are several merits in the KKR Green's function method, compared to other first-principles approaches. The most important advantage is the ability to perform the calculations of alloys and impurity doped systems, combining with the coherent potential approximation (CPA). Additionally, since the Green's function is directory calculated in this method, physical quantities, e.g., magnetic exchange interactions and transport properties, can be efficiently calculated by the linear response theory.

Automatic high-throughput calculations by

first-principles approaches are not easy tasks, because we need to appropriately control many numerical parameters and self-consistent procedures. For example, in the KKR Green's function method, the energy integration of the Green's function is performed in the complex energy plane to obtain the electron density. This complex energy contour must cover the valence bands and depends on systems. Our python interface for the high-throughput calculations enable to determine the numerical parameters and to manage the self-consistent procedures completely automatically. For the electronic structure calculations, the AkaiKKR program package is employed.

The automatic high-throughput calculations have been demonstrated for quaternary high entropy alloys with BCC and FCC solid solution phases, where 4 principal elements have the same atomic concentration and are randomly distributed in the crystals. The number of the target elements are 38 as follows: Al, Si, Sc, Ti, V, Cr, Mn, Fe, Co, Ni, Cu, Zn, Ga, Ge, Y, Zr, Nb, Mo, Tc, Ru, Rh, Pd, Ag, Cd, In, Sn, Hf, Ta, W, Re, Os, Ir, Pt, Au, Hg, Tl, Pb and Bi. We randomly choose the 4 elements from the above target elements and construct a quaternary high entropy alloy. Since both the BCC and FCC cases are considered, the total number of the systems is 147,630. All calculations are done by the ISSP supercomputer, system B.

We succeeded in automatically converging 99.99% of the systems, i.e., 147614/147630.

Figure 1 shows a part of our high-throughput calculations, in which the magnetic moments and Curie temperatures for the quaternary high entropy alloys with the BCC phase are plotted. The Curie temperatures are calculated by the magnetic exchange interactions and mean-field approximation. Such database is quite useful for the design of new functional materials. For example, in the cases of high-performance soft magnets, the high magnet moments and Curie temperatures are needed. Using the database, we can screen the candidate systems immediately. Here, it is concluded that FeCoXY, FeCoNiY, and MnFeCoY systems are good candidates for the high-performance soft magnets

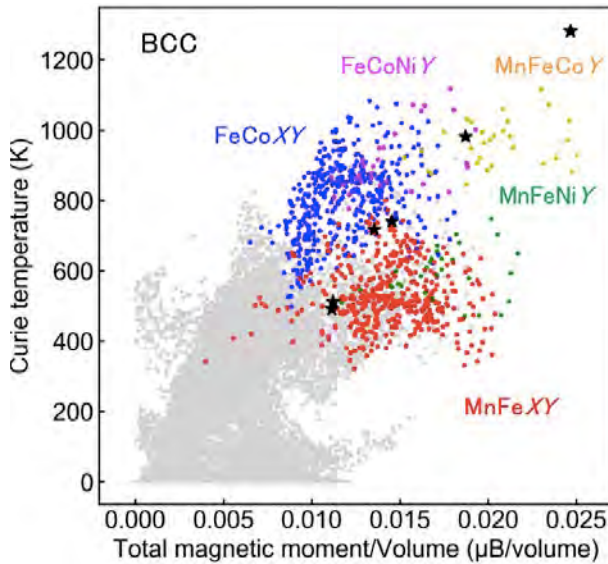


Figure 1: Automatic high-throughput calculations for quaternary high entropy alloys with the BCC phase.

References

- [1] T. Fukushima, H. Shinya, A. Masago, K. Sato and H. Katayama-Yoshida: Appl. Phys. Exp. **12** (2019) 063006.
- [2] S. Yamada, S. Kobayashi, A. Masago, L. S. R. Kumara, H. Tajiri, T. Fukushima, S. Abo, Y. Sakuraba, K. Hono, T. Oguchi,

and K. Hamaya: Phys. Rev. B **100** (2019) 195137.

- [3] A. Masago, H. Shinya, T. Fukushima, K. Sato, and H. Katayama-Yoshida: AIP Advances **10** (2020) 025216.
- [4] T. Nunokawa, Y. Fujiwara, Y. Miyata, N. Fujimura, T. Sakurai, H. Ohta, A. Masago, H. Shinya, T. Fukushima, K. Sato, and H. Katayama-Yoshida: J. Appl. Phys. **127** (2020) 083901.

Electron Theory on Secondary-Battery Materials

Hiroki KOTAKA¹, Motoyuki HAMAGUCHI², Huu Duc LUONG²,
Hiroyoshi MOMIDA^{1,2}, Tamio OGUCHI^{1,2}

¹*ESICB, Kyoto University, Katsuragoryo, Kyoto, Kyoto 615-8245*

²*ISIR, Osaka University, Mihogaoka, Ibaraki, Osaka 567-0047*

Microscopic mechanism of charging and discharging reactions in several battery systems is studied by first-principles calculations to explore novel secondary battery materials. In this year, we further extended our previous studies on Na/NaFeSO₄F and Li/Li_{2+2x}Mn_{1-x}Ti_{1-x}O₄ systems.

Recently NaFeSO₄F has been expected to be a candidate cathode material for the next-generation Na secondary batteries. In this first-principles study [1], the structural stability and voltage-capacity profiles of Na/NaFeSO₄F system are investigated. Calculated total energy of NaFeSO₄F is compared with those of NaF and FeSO₄ and found to be slightly stable to the phase separation. X-ray absorption spectroscopy (XAS) spectra at the K-edges of Fe, Na, and F for NaFeSO₄F and FeSO₄F in the fully discharged and charged states and of NaF and FeSO₄ are computed with the Fermi golden rule within the electric dipole and quadrupole approximation. The XAS spectra at Fe K-edge reveal that the discharged state in NaFeSO₄F and the charged state in FeSO₄F are dominated by Fe²⁺ (*d*⁶) and Fe³⁺ (*d*⁵), respectively. It is also found that the XAS spectra near K-edge of F in addition to Fe provide crucial information concerning the local structure in the relevant phases existing during the reaction processes.

Li-excess cation-disordered rock-salt oxides Li_{2+2x}Mn_{1-x}Ti_{1-x}O₄ have recently attracted much interests as high-capacity cathodes associated with two-electron reactions. In these oxides, cations are disordered on the octahedral

sites coordinated by six oxygen ions and the octahedra are expected to be stable during discharging and charging reactions. To clarify the mechanism of the reactions, cathode properties of the oxides with the Li-excess of $0 \leq x \leq 0.3$ are investigated by using first-principles calculations [2]. To evaluate the structure stability and reaction equations of the cathode materials for each *x*, formation enthalpies of Li_{2+2x-y}Mn_{1-x}Ti_{1-x}O₄ are calculated as a function of Li-removal amounts *y* considering several Li configurations. To model the oxides with disordered cations and several Li concentrations *x* and *y*, supercells including 80 atoms of rock-salt lattice are assumed with the special quasi-random structure method. Based on the estimated reaction equations, voltage-capacity profiles are obtained for each *x* and compared with experiments. By analyzing the electronic structures, roles of cation and anion redox reactions depending on *y* as well as *x* are discussed in detail. We discuss energy stability of O₂-release from the cathode during charging/discharging processes by calculating vacancy formation energies of O and Li. The best *x* values in terms of voltages, capacities, and stability against the O₂-releases are proposed.

References

- [1] H. Momida *et al.*, *J. Phys. Soc. Jpn.* **88**, 124709 (2019).
- [2] M. Hamaguchi, *et al.*, *Electrochimica Acta* **330**, 135286 (2020).

Ab initio studies toward functional nanomaterials based on abundant elements

Tetsuya TAKETSUGU

Faculty of Science, Hokkaido University

N10W8, Sapporo, Hokkaido 060-0810

Ab initio studies on various nano materials are important to understand and design new functional materials with abundant elements for reducing costs and dependences on precious metals used in many important aspects in our daily lives and therefore toward sustainable society. Heterogeneous catalysts rely mostly on the expensive and rare metals such as Pt, Rh, Pd, or Ru in automotive gas exhausts control, water gas shifts, fuel cells, as well as combus- tive decomposition of ammonia. Platinum and palladium are also used for hydrogen based energy strategies. Due to their high cost and limited amounts, to reduce or even replace these metals is emergent issues in industry. To that end, we perform density functional theory (DFT) computations under the periodic boundary conditions together with projector augmented wave method with VASP using ISSP supercomputers to gain chemical insights to understand the chemical mechanisms in conventional catalysts as well as to design novel catalysts with abundant elements.

We have developed a surface adsorption model calculation database toward application to activity prediction of heterogeneous catalysts [1], where band calculations with SIESTA are performed for various pure and alloy metal surfaces adsorbed with molecules and atoms relevant to important catalysis such as water gas shift. As a new functional nanomaterial, we have studied structural and electronic properties of borophene, an artificial two-dimensional materials, whose structural

and electronic properties are not typical for their bulk counterparts [2]. Scanning tunneling microscopy and density functional theory calculations show that this structure forms as a single phase on iridium substrate in a wide range of experimental conditions and maybe then decoupled from the substrate via intercalation. We foresee that the adjacent borophene sites with opposite electron doping might exhibit catalytic activity or facilitate highly regular adsorption of large molecules, metal clusters, and other objects interesting for catalysis, sensors, and nanotechnology.

The excited states dynamics and spectroscopy are also important for the study on functional nanomaterials. For spectroscopy, the roles of silver nanocluster and plasmonic nanocavity for surface- and tip-enhanced Raman spectroscopies, respectively, are investigated [3,4]. We are further studying electronic excitations of small molecule excited by spatially nonuniform electric field, namely the near-field, by using the real-time time-dependent density functional theory codes such as SALMON.

References [1] M. Kobayashi, H. Onoda, Y. Kuroda, and T. Taketsugu, *J. Comput. Chem. Jap.*, 18, 251-253 (2019). [2] N. A. Vinogradov, et al, *ACS Nano*, 13, 14511-14518 (2019). [3] T. Tsuneda, T. Iwasa, and T. Taketsugu, *J. Chem. Phys.*, 151, 094102 (2019). [4] R. B. Jaculbia et al., *Nature Nanotechnology*, 15, 105-110 (2020).

Development of high-performance permanent magnets by large-scale simulation and data-driven approach

Takashi MIYAKE

CD-FMat, AIST

Umezono, Tsukuba, Ibaraki 305-8568

We have studied magnetic properties and stability of rare-earth magnet compounds using first-principles calculation combined with machine-learning techniques. The $R\text{Fe}_{12}$ -type compounds having the ThMn_{12} structure have attracted attention in recent years, because high saturation magnetization can be expected from their high iron concentration. $\text{NdFe}_{12}\text{N}_x$ and $\text{Sm}(\text{Fe},\text{Co})_{12}$ films have successfully synthesized a few years ago, and it was reported experimentally that these compounds have higher saturation magnetization, higher anisotropy field and higher Curie temperature than $\text{Nd}_2\text{Fe}_{14}\text{B}$ which is the main phase of the neodymium magnet. However, they are thermodynamically unstable, and partial substitution of Fe sites are necessary to stabilize a bulk phase. The choice of rare-earth element also affects stability [1].

We calculated the magnetization, Curie temperature and formation energy of $(R_{1-\alpha}Z_{\alpha})(\text{Fe}_{(1-\beta)(1-\gamma)}\text{Co}_{\beta(1-\gamma)}\text{Ti}_{\gamma})_{12}$ ($R=\text{Nd}, \text{Sm}, \text{Y}, Z=\text{Zr}, \text{Dy}$) based on density functional theory using Akai-KKR code. Non-stoichiometric composition is treated by the coherent potential approximation. Intersite magnetic exchange couplings are calculated by Liechtenstein's method, from which the Curie temperature is evaluated by solving the derived Heisenberg model in the mean-field approximation. To reduce the systematic error in the formation energy obtained by the KKR-CPA, data integration method (Fig.1)

is adopted, where the formation energies of stoichiometric systems calculated by QMAS are used to reduce the systematic error.

In order to determine the optimal composition efficiently, we adopt Bayesian optimization. We performed 1000 independent runs to evaluate the success rate statistically. Figure 2 shows the success rate of finding top 10 systems out of 3630 chemical compositions within 50 trials. The target variables are saturation magnetization, Curie temperature and formation energy. The success rate is over 95 % if we appropriately chose the descriptor, which is much higher than that by the random sampling (12.9%).

References

- [1] Yosuke Harashima, Taro Fukazawa, and Takashi Miyake: *Scripta Materialia* **179** (2020) 12.
- [2] Taro Fukazawa, Yosuke Harashima, Zhufeng Hou and Takashi Miyake: *Phys. Rev. Mater.* **3** (2019) 053807.

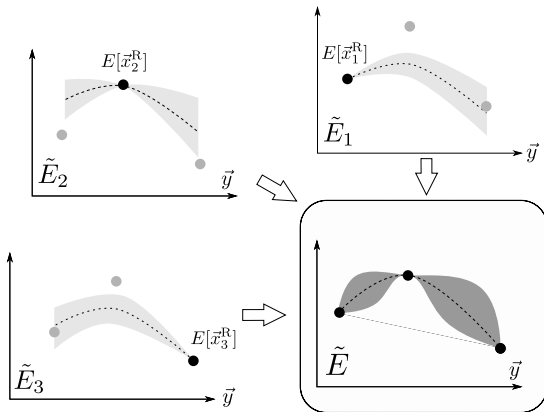


Figure 1: Data integration method, where systematic errors contained in a large number of data for non-stoichiometric compositions are corrected by a small number of more accurate data for stoichiometric compositions.

[2].

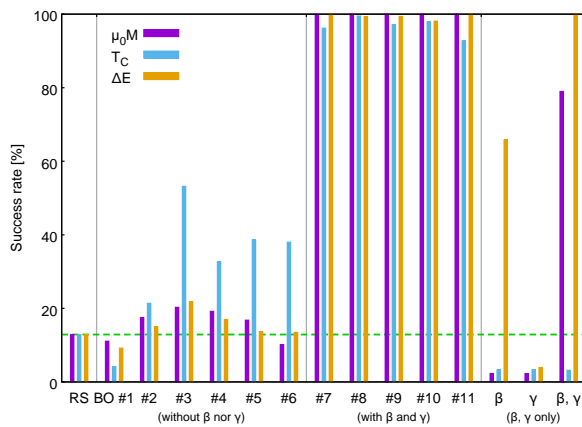


Figure 2: Success rate of finding the system with the top 10 values of magnetization, Curie temperature and formation energy out of 3630 candidates within 50 trials [2].

Multiscale simulations on complex multiphase flows

Youhei Morii, Takahiro Murashima, and Toshihiro Kawakatsu

Department of Physics, Graduate School of Science, Tohoku University, Sendai 980-8578

We developed multiscale simulation techniques (MSS) [1] and a multiscale simulation platform for complex fluids (MSSP) [2,3], under the support from Post-K project and HPCI. These MSS and MSSP are aimed to apply for complex flow phenomena such as multiphase flows and viscoelastic flows whose constitutive equations are not a priori known. In such systems, a simple model constitutive equation is not in general available, and therefore one must obtain the stress tensor from the flow history of the fluid. As such a flow is often non-Markovian, Lagrangian description is quite suitable to trace the flow history. Smoothed particle hydrodynamics (SPH) is a typical simulation technique of fluid flows based on Lagrangian description. Our MSSP is based on this SPH method, where each SPH particle contains a microscopic simulator inside

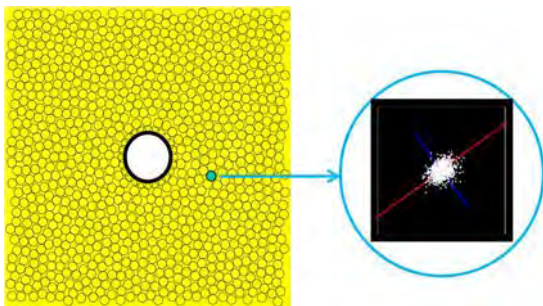


Fig.1 A schematic illustration of MSSP.

it (See Fig.1). The instantaneous stress that drives the macroscopic flow is calculated using this microscopic simulator.

We applied this technique to a viscoelastic polymeric fluid flowing around a cylindrical obstacle that generates Karman's vortex street. Figure 2 shows a comparison between (a) a Newtonian fluid and (b) a Maxwellian fluid that contains set of dumbbells as a model of polymer solution. One can confirm the effect of viscoelasticity coming from the polymer component on the Karman's vortex street.

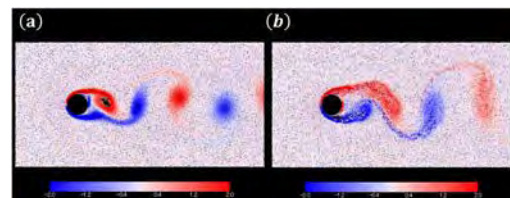


Fig.2 Karman vortex street for (a) a Newtonian fluid and (b) a Maxwellian fluid.

References

- [1] T. Murashima, S. Urata, S. Li, *Eur. Phys. J. B*, 92, 211 (2019).
- [2] 森井洋平, 川勝年洋, 第 68 回高分子討論会, 福井大学 文京キャンパス, 2019/9/25.
- [3] Youhei Morii, Toshihiro Kawakatsu, 10th International Conference of the Asian Consortium on Computational Materials Science (ACCMS-10), Hong Kong, 2019/7/24.

Order-disorder transition in the superhigh-pressure phase of Mg_2SiO_4

Koichiro UMEMOTO

Earth-Life Science Institute,

Tokyo Institute of Technology, 2-12-1 Meguro-ku, Ookayama, Tokyo 152-8550

MgSiO_3 bridgmanite with the orthorhombic perovskite structure is a major constituent of the lower mantle of the Earth. It takes the post-perovskite (PPV) structure near the core-mantle boundary pressure (~ 125 GPa). The PPV phase is the final form of MgSiO_3 in the Earth. However, at much higher pressures in “super-Earths” which are exoplanets expected to be terrestrial with masses much larger than the Earth, MgSiO_3 PPV should undergo “post-PPV” transitions. So far, first principles studies have predicted the three-stage dissociation of MgSiO_3 PPV: MgSiO_3 PPV \rightarrow I-42d-type Mg_2SiO_4 + P2₁/c-type MgSi_2O_5 \rightarrow Mg_2SiO_4 + Fe₂P-type SiO_2 \rightarrow CsCl-type MgO + SiO_2 [1,2]. When MgSiO_3 coexists with NaCl-type MgO or pyrite-type SiO_2 , they were predicted to recombine into Mg_2SiO_4 or MgSi_2O_5 [3]. Transition pressures of these post-PPV transitions are extremely high, $>\sim 500$ GPa, and have been still difficult to be achieved experimentally. These predictions were based on the lowest-enthalpy phases under ultrahigh pressures. Temperature effects by phonon were taken into account by using the quasi-harmonic approximation (QHA). These post-PPV

transitions and thermodynamic quantities calculated for these phases have been already used in numerical modeling of mantle dynamics of super-Earths [5].

In this study, we predicted order-disorder transition in the cation sublattice of tetragonal Mg_2GeO_4 by first principles [4]. Mg_2GeO_4 is a candidate of low-pressure analog of Mg_2SiO_4 . The dissociation of MgGeO_3 PPV into pyrite-type GeO_2 and I-42d-type Mg_2GeO_4 was predicted to occur at ~ 170 GPa [5]. Therefore, Mg_2GeO_4 is a useful system to study the post-PPV transitions experimentally. In Mg_2GeO_4 and Mg_2SiO_4 , local oxygen arrangements around Mg and Ge atoms are very close to each other. Therefore, configuration entropy is expected to induce the order-disorder transition at high temperature.

The order-disorder transition temperature (T_c) is given by the peak temperature of the heat capacity which is calculated from the partition function with respect to cation configurations. For Mg_2GeO_4 , we constructed a supercell consisting of 56 atoms and generated cation configurations until the convergence of T_c was achieved. Then we predicted that the

order-disorder transition should occur at ~ 3000 K and 200 GPa; this pressure-temperature condition is now achievable by the diamond-anvil-cell experiments. We found that T_c increases with pressure. Across the transition, the symmetry of Mg_2GeO_4 increases from tetragonal (I-42d) in the ordered phase to cubic (I-43d) in disordered one. In fact, the crystal structure of the disordered cubic phase is identical to that of Th_3P_4 . We also clarified that the effect of phonon on this transition is very small within the QHA.

Since Mg_2GeO_4 is the low-pressure analog of Mg_2SiO_4 , the order-disorder transition predicted in this study is expected to occur also in Mg_2SiO_4 and will play an important role in modeling interiors of super-Earths.

The first principles calculations in this study were performed using the Quantum-Espresso package (<https://www.quantum-espresso.org>) on the supercomputer (system B) at the

Institute for Solid State Physics. This research was supported by MEXT as “Exploratory Challenge on Post-K computer” (Challenge of Basic Science – Exploring Extremes through Multi-Physics and Multi-Scale Simulations)

References

- [1] S. Q. Wu, et al.: J. Phys.: Condens. Matter **26** (2014) 035402.
- [2] H. Niu et al.: Sci. Rep. **5** (2015) 18347.
- [3] K. Umemoto et al.: Earth Planet. Sci. Lett. **478** (2017) 40.
- [4] K. Umemoto and R. M. Wentzcovitch: in preparation.
- [5] A. P. van den Berg, et al.: Icarus **317** (2019) 412.
- [6] K. Umemoto and R. M. Wentzcovitch: Phys. Rev. Mat. **3** (2019) 123601.

Chain-Increment Method for Approaching the Chemical Potential of a Polymer with All-Atom Model

Kazuo YAMADA and Nobuyuki MATUBAYASI

Division of Chemical Engineering, Graduate School of Engineering Science,

Osaka University, Toyonaka, Osaka 560-8531

We have computed the free energy of the dissolution of the polymer in polymer binary systems [1] using all-atom molecular dynamics simulations. An atomistic computation of free energy is a challenging task, however, when a polymer molecule is treated simultaneously as a whole. This is because a polymer is highly flexible and structurally diverse due to large number of intramolecular degrees of freedom. Given the fundamental and practical importance of the chemical-potential calculation of polymer, therefore, an elaborate scheme needs to be established which exploits a specific nature of the polymeric structure.

We develop a chain-increment method to approach the chemical potential of a polymer with all-atom model. The intermolecular interaction of a polymer of interest with the surrounding molecules is introduced sequentially for the monomers, and the free energy for turning on the interaction is treated within the framework of the energy-representation theory of solutions. In our method, we compute the free energy of chain increment $\Delta\mu_i^{\text{incr}}$ along the monomers in the tagged polymer as well as the total free energy $\Delta\mu$ of the

polymer as a sum of $\Delta\mu_i^{\text{incr}}$ over the monomers in the tagged polymer. In the present report, we focus on the computation of the incremental free energy in polymer-melt systems [1].

The polymer species treated are polyethylene (PE), polypropylene (PP), poly(methyl methacrylate) (PMMA), and polyvinylidene difluoride (PVDF) in their linear forms. All-atom molecular dynamics simulations and free-energy calculations have been implemented on the supercomputer system at ISSP. The free energy of chain increment is shown in Fig. 1 at the number of monomer units of 100. The incremental free energy $\Delta\mu_i^{\text{incr}}$ is obtained for each monomer by using the scheme in [1], and it is found that the incremental free energy stays constant within 0.1 kcal/mol except at terminals. The standard deviation is within 0.2 kcal/mol in the inner part of the polymer, and the averaged free energy of chain increment is insensitive to the chain length. All-atom computation is thus feasible for the free-energy analysis of a polymer system at the degree of polymerization of several tens or more. It is also seen that the preference order of $\Delta\mu_i^{\text{incr}}$ agrees with that of the average interaction energy $\langle u \rangle_i$ of the

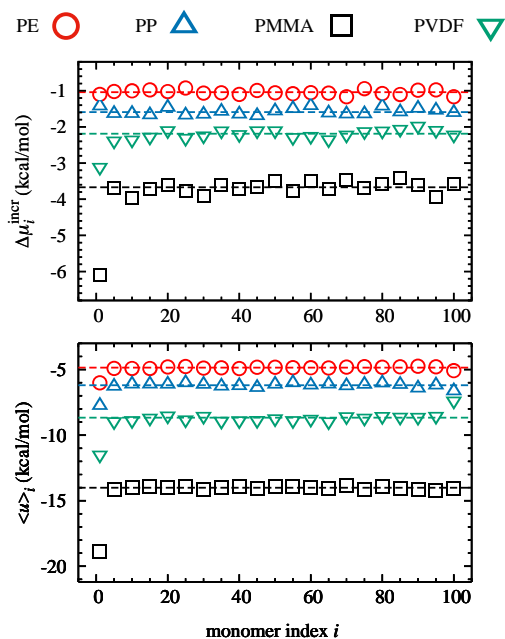


Fig 1: Incremental free energy and the average interaction energy against the index i of the incremented monomer in the tagged polymer. The degree of polymerization is 100 in this figure, and $\Delta\mu_i^{\text{incr}}$ and $\langle u \rangle_i$ are plotted against the monomer index at $i = 1, 5, 10, 15, \dots, 90, 95, \text{ and } 100$. The horizontal, dashed line is the averaged value of $\Delta\mu_i^{\text{incr}}$ or $\langle u \rangle_i$ over $i = 5, 10, 15, \dots, 90, \text{ and } 95$.

incremented monomer with the surroundings.

We further compute the total solvation free energy $\Delta\mu$ as a function of the degree of the polymerization N for PE and PMMA, by using the incremental free energy of solvation $\Delta\mu_i^{\text{incr}}$ at $i = 1, 5, 10, \dots, (N-10), (N-5), \text{ and } N$. In Fig. 2, a good linearity of $\Delta\mu$ to N is observed. The free energetics of a long polymer is thus determined by the chain-increment contribution $\Delta\mu_i^{\text{incr}}$, and Figs. 1 and 2 demonstrate that $\Delta\mu_i^{\text{incr}}$ can be assessed from an all-atom simulation with the

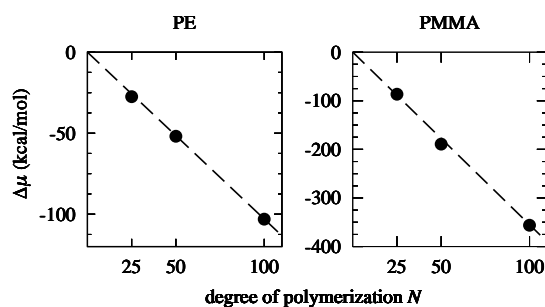


Fig 2: Total solvation free energy $\Delta\mu$ against the degree of polymerization N at 25, 50, and 100 for PE and PMMA. $\Delta\mu$ is estimated from $\Delta\mu_i^{\text{incr}}$ at $i = 1, 5, 10, \dots, (N-10), (N-5), \text{ and } N$. The dashed line is the least-square fit to the form of $\Delta\mu \propto N$, and the slope is -1.0 and -3.6 kcal/mol for PE and PMMA, respectively.

degree of polymerization of several tens or more.

Atomistic computation of the chemical potential is of much computational demand for a polymer when the interaction with the solvent is turned on simultaneously throughout the whole polymer. The method of chain increment is an alternative scheme that introduces the interactions sequentially along the polymer chain. This work formulates an all-atom method for chain increment by combining molecular simulation with the energy-representation theory of solutions, and it is demonstrated that the free energy of chain increment can be obtained at a precision of a few tenths of kcal/mol.

References

- [1] K. Yamada and N. Matubayasi: Macromol. **53** (2020) 775-788.

Study on thermodynamic properties and NO_x redox reactions of ternary alloy nanoclusters by O(N) density functional calculations

Shih-Hsuan Hung and Taisuke Ozaki

Institute for Solid State Physics, University of Tokyo

Kashiwa-no-ha, Kashiwa, Chiba 277-8581

We perform first-principles calculations and Monte Carlo sampling to investigate the structures of ternary PdRuM (M=Pt, Rh, or Ir) nanoparticles (NPs) with respect to three different spherical shapes. The calculation is carried out using OpenMX (Open source package for Material eXplorer) software package.

1 Introduction

Metallic nanoparticles (NPs) are a promising functional material in many aspects, such as energy conservation, catalyst, and elements storage. [1] To achieve better performance of particular functions, many experiments synthesize modified NPs to adjust their properties physically and chemically. Bimetallic PdRu NPs have been reported for providing better catalytic reactions, but the drawback is suffered from the loss of metal element during catalytic cycles. [1, 2] Therefore, PdRuPt, PdRuRh, and PdRuIr NPs or alloy have been studied and demonstrate their promising ability of NO reaction. [4, 3] Therefore, we would like to investigate these NPs and provide deeper insight in atomistic aspect.

2 Result

To compare different morphology influencing different composition ternary NP, we select three different spherical shapes for the NPs. There are hexagonal close-packed (hcp),

truncated-octahedral (fcc), and icosahedral (fcc) shapes with 57, 55, and 55 atoms, respectively. To achieve higher coverage of energy survey, each nanoparticle is sampled 30 times using Monte Carlo sampling method, thus there is 270 sampling in total. The statistical characteristic implies the position trend of individual atom for respective nanoparticles (detail is in published paper). By following the trend, we manually construct the bare ternary NPs and find the most stable one. Figure 1 shows the most stable ternary NPs in our calculation. The calculation shows that the atomic arrangements depend on the surface formation energy of individual elements. In other words, the element possesses smaller surface formation energy dominating the surface sites. The species have greater surface formation energy immerse in the NPs as bulk-like state. Figure 1 demonstrates Ru atoms are always as a core in NPs due to its larger surface formation energy ($\gamma = 1.31$ eV/atom) of fcc (111) surface. In addition, there are two particular shells are found in the investigation. One configuration is binary solid solution alloy and the other one represents that two elements segregate from each other on the shell. The reason of these two particular arrangements is because the NPs tend to minimize its surface strain, compared to lattice constant of Pd fcc bulk (3.79 Å). For the NPs with solid solution shell, the Pd-M bond length decreases by 3.8 % in average. Meanwhile, the bond reduc-

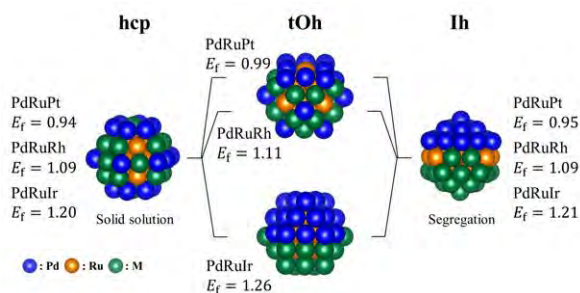


Figure 1: The most energetically stable ternary PdRuM NPs in the calculations. The unit of E_f is eV/atom.

tion of 3.0 % in average has been found for the configurations with segregation shell. In addition, the Ir-Ir bond length shows a significant reduction of 6.2 %. By modeling the single layer hexagonal as shell structure, the calculation shows a good agreement with our NPs calculation. The reduced bond length of alloy decreases the total calculated energy.

Oxidized NPs is an other problematic issue of catalyst. Due to the oxidation formation energy variance, the elements of the NPs may migrate from site to site. The oxygen adsorption on surface calculation demonstrates that the preference of oxygen adsorption (eV/atom) on fcc hollow site is found to be Ru (-3.65) \rightarrow Rh (-2.78) \rightarrow Ir (-2.47) \rightarrow Pd (-2.06) \rightarrow Pt (-1.84). Besides the single oxygen adsorption on cleaved surface, we examine the oxygen molecule adsorption on pure Pd NPs. The calculation demonstrate that the oxidation energy is as a function of O-O distances. The increasing O-O distance up to 5.0 Å decreases the oxidation formation energy. Figure 2 demonstrates the most stable oxidized ternary NPs and their oxidation formation energy what we can find. The result shows that the Ru atoms migrate outward to the surfaces of NPs to be oxide. Pt, Pd and Pd atoms penetrate inwards as a core of the ternary PdRuPt, PdRuRh, and PdRuIr NPs, respectively. By calculating the NPs formation energy with respect to chemical potential of oxygen molecule, the free energy indicates hcp ternary NP is thermodynamically

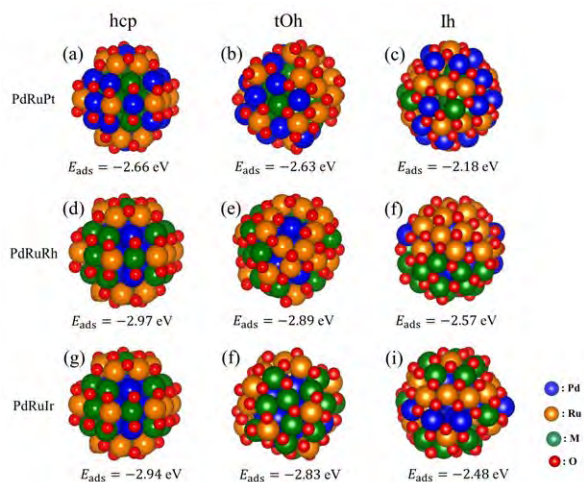


Figure 2: The most energetically stable structures of high oxygen coverage on hcp, tOh, and Ih ternary NPs.

cally unstable under oxygen-rich condition.

3 Conclusion and Discussion

In summary, we have provide deeper insight into the most stable structures with three different morphologies and two oxidation statuses. The investigation shows the atoms are organized in specific arrangement instead of solid solution alloy. In addition, the oxidation condition can facilitate the atomic migration in the ternary NPs. Although the scale of the study is not satisfying to interpret real situation, it can be a pilot investigation for real scale NPs calculation and provide some possible configurations in advance.

References

- [1] Kusada Kohei et al.: *J. Am. Chem. Soc.* **136** (2014) 1864–1871
- [2] Wu Dongshuang et al.: *Phys. Chem. Chem. Phys.* **14** (2012) 8051–8057
- [3] Sarker Md Samiul et al.: *J. Mater. Res.* **29** (2014) 856–864
- [4] Shang Changshuai et al.: *Nano Res.* **11** 2018 4348–4355